Modeling optical properties of plant epicuticular wax

Eugene Bukhanov
Kirensky Institute of Physics SB RAS
Krasnoyarsk, Russia
k26Tony@ya.ru

Yuru Gurevich
FRC KSC SB RAS
Krasnoyarsk, Russia
Btchem@mail.ru

Mikhail Krakhalev
Kirensky Institute of Physics SB RAS
Krasnoyarsk, Russia
kmn@iph.krasn.ru

Dmitry Shabanov
Kirensky Institute of Physics SB RAS
Krasnoyarsk, Russia
Hio123123@mail.ru

Abstract—**Wax is found on the leaves almost of all plants. Its physicochemical and protective properties are widely discussed in the scientific literature. In the presented work, the influence of the structure of wax on the optical properties in wheat leaves and needles of blue spruce has been revealed for the first time. Long-period ordering was established. The structural elements are nanotubes up to several microns in length and about 150 nm in diameter. The paper presents the influence of a long-period structure on the optical properties and local characteristics of light waves, including the transmission spectrum, the density of photon states, as well as fluorescence spectra and polarization microscopy. Using modern mathematical tools, the main spectral and optical characteristics were calculated using the example of the wax cover of blue spruce and glaucas wheat. Based on calculations that establish the relationship between the structural, spectral and optical properties, the influence of wax structures on the process of photosynthesis was revealed.**

Keywords—**photonic crystal, epicuticular wax, density of photon states, fluorescence**

I. INTRODUCTION

The wax on the surface of plants has an extremely important role. It repels moisture from nutrients, thereby preventing them from contamination by bacteria and mold. Moreover, it is an excellent preservative. On the other hand, it protects plant cells from excessive loss of water and strong light effects [1]–[6], especially in the field o f u ltraviolet r adiation, their destructive effect on photosynthetic organelles. A wide range of actions is due not only to the chemical properties of wax, to a greater extent by its structural features [7]–[12], easily changing under the influence o f e xternal mechanical, thermal and light influences. Surprisingly, waxes are composed of conglomerates of long-period hydrocarbons, acids, and alcohols. As a rule, the length of their chains is more than 20 lengths of C-C bonds. The quantitative ratios of similar acids and alcohols are not the same in different plant species. But there are few fluvonoids i n e picuticular w axes, although this group of chemical compounds are produced by plants in sufficient q uantities. P lant p olyphenols h ave a number of properties that aldehydes and ketones provide in wax.

Among them are pigments, antioxidants. Unlike wax-forming chemical compounds, their structures are not flexible and are less susceptible to external physical and chemical influences. For this reason, there is reason to believe that the unique properties of wax are mainly due to structural features. It has a number of amazing properties: with a high flexibility of polymer chains of their chemical diversity, a structure with a large order parameter is formed [7]–[12]. The self-formation of such structures was studied in detail in [13]–[17], while studies were carried out on the transformation spectrum in a free state and under external influences. Interesting results were obtained in elucidating the role of the substrate on polar substrates. The orientation of the crystal axes differs from the orientation of the analogous axes of crystals grown on nonpolar substrates; in the latter case, the structure is less ordered. In [18]–[20], spiral twisted structures were found. They naturally have the effect of chirality, with the sign and properties of photonic crystals, since the pitch of the spiral strongly depends on temperature and in a certain temperature range it becomes comparable to the wavelength of light. In this case, the color of the reflected light depends not only on the presence of pigments, but to a greater extent on the pitch of the spiral. In this case, the ratio of the amplitudes and phases of the electric and magnetic fields is preserved, which ensures the diffraction of light on a smooth gradient caused by the rotation of the optical axis. In ordinary photonic crystals, diffraction is due to the different refractive indices of the media from which the photonic crystal is made. The required parameters can be achieved by selecting materials with different refractive indices and different layer thicknesses.

The uniqueness of the photonic-crystal material created by nature is that a homogeneous material is used, no unnecessary contaminating elements are introduced. The color caused by structural features is usually called the structural color, in contrast to the chemical color caused by the pigment of the molecules. Structural coloration changes with changing viewing angle. The contrast is not maximal, since the helicoidal

structure reflects only one of the two circular polarizations of the light wave. This problem in nature is solved no less elegantly. Alternating left- and right-handed helicoidal structures are used [13], [21]–[23]. In it, the interference periodically repeating forms reflection bands in the spectrum of transmitted light. In the case of an infinite crystal, such frequency ranges can form photonic bandgaps. No less interesting, both from a theoretical and a practical purpose, is the study of the influence of defects in the wax structure on the optical characteristics of the sheet.

The aim of this research was to study the optical properties of epiticular waxes in the needles of blue spruce and glaucas wheat.

II. MATERIALS AND METHODS

A. Wax isolation

A unique method of obtaining samples of wax and pine needles from spruce and glaucas wheat was used in the work. The difficulty lies in the need to separate the layer of waves without damaging its structural characteristics. The mechanical separation is too coarse, even by eye you can see a change in shape, which, of course, is associated with a change in the microstructure. Any chemical attack also leads to inhomogeneous salting out and naturally a change in the microstructure. Therefore, we used the properties of water to penetrate deeply into wax structures under the action of van der Waals forces and expand when frozen. For this, clean needles and leaves, on which a blue color or gray-blue for wheat is visible over the entire surface, which indicates the integrity of the epiticular wax, was placed in a vessel with distilled water. The exposure time for different samples varied from 5 to 24 hours. Subsequently, the temperature was gradually reduced by no more than one degree per hour to minus 20° C. At this temperature, the water froze not only in volume, but also in the pores of the wax. Then heating was carried out. It turned out that heating can be carried out in a more accelerated version: 15 degrees in 1 hour. After thawing, smooth wax plates float to the surface and were collected on substrates. Three types of substrates were used: metal for examining samples by high-resolution electron microscopy, quartz for measuring optical characteristics, and glass with an electrically conductive layer.

Research as a substrate on glass with a conductive layer allows measurements to be carried out on one sample by various methods (electron microscopy, optical measurements). But the use of quartz substrates and metal allows you to obtain more accurate parameters. The reasons for the floatation of the wax plates are due to the fact that their bulk density is less than the density of water. They are hydrophobic, the energy of interaction with water is less than that of interaction with quartz or metal, therefore, without distorting the structure, they are deposited on metal and quartz substrates.

B. Microscopy

The morphological and structural characteristics of the isolated wax were studied using SEM on a Hitachi SU3500 microscope (accelerating voltage 10 kV, W-cathode) and high-resolution TEM Hitachi S-5500 (accelerating voltage 30 kV, field emission cathode).

Due to the absence of chemically active impurities, there is every reason to assume that images of the structure using electron microscopy have minimal distortion.

Wax plates were optically observed in transmitted and reflected light using an Axio Imager.A1m (Zeiss) microscope and a 50x/0.8 lens. The observations were carried out in non-polarized and polarized light in the geometry of crossed polarizers.

C. Calculations

In this work, we calculated the transmission spectra and the density of photon states of various periodic structures with low contrast (corresponding to plants).

Calculation of the spectral characteristics of the model structures of leaf epicuticular waxes. In a medium consisting of two materials of thickness d and d and refractive indices n and . Selective reflection of the light wave can also be achieved using multilayer structures.

$$2(n_1 d_1 \cos\theta_1 + n_2 d_2 \cos\theta_2) = m\lambda \qquad (1)$$

The optical response of arbitrary multilayer structures is calculated using the transfer matrix method. A similar selective reflection can be obtained for objects consisting of the same material but having a spiral structure. An example of such a substance is a cholesteric liquid crystal [24].

As you can see, periodic materials with selective reflection are morphologically different and often occur in nature [25], [26]. Moreover, their role and significance for photosynthesis have not been studied enough.

Let us consider in more detail the propagation of light in a medium consisting of layers of thickness Z_N and having a refractive index n_N.

Let a plane electromagnetic wave propagate along the Z axis. The structure is periodic with a period d with two sublattices with refractive indices n1 and n2.

The amplitudes of waves (A and B) traveling in the right and left directions, respectively, in the previous layer depend on the same values in the current one:

$$A_{N-1} = \frac{1}{2}((1 + \frac{n_N}{n_{N-1}})A_N e^{-i\frac{\omega}{c}n_N L_N} +$$
$$+ (1 - \frac{n_N}{n_{N-1}})B_N e^{i\frac{\omega}{c}n_N L_N}) \qquad (2)$$

$$B_{N-1} = \frac{1}{2}((1 - \frac{n_N}{n_{N-1}})A_N e^{-i\frac{\omega}{c}n_N L_N} +$$
$$+ (1 + \frac{n_N}{n_{N-1}})B_N e^{i\frac{\omega}{c}n_N L_N}) \qquad (3)$$

For TE-wave (electrical component perpendicular to the plane of incidence):

$$E(z, N) = A_N^{TE} e^{-ik_N z} + B_N^{TE} e^{ik_N z} \qquad (4)$$

$$H(z, N) = ik_N(A_N^{TE}e^{-ik_Nz} - B_N^{TE}e^{ik_Nz}) \quad (5)$$

$$C = \frac{k_N}{k_{N-1}} \quad (6)$$

For TM wave:

$$H(z, N) = A_N^{TM}e^{-ik_Nz} + B_N^{TM}e^{ik_Nz} \quad (7)$$

$$E(z, N) = i\frac{n_N^2}{k_N}(A_N^{TM}e^{-ik_Nz} - B_N^{TM}e^{ik_Nz}) \quad (8)$$

$$C = \frac{k_{N-1}n_N^2}{k_N n_{N-1}^2} \quad (9)$$

$$k_N = \frac{\omega}{c}\sqrt{n_N^2 - n_0^2\sin^2\theta} \quad (10)$$

where Z is a variable local to each layer, the origin for it is placed on the right border of the layer; θ is the angle of incidence of the beam from the external environment.

At normal incidence of light $k_N = \omega n_N/c$, expressions (4-6) and (7-10) become identical.

Knowing that only an outgoing wave exists at the exit from the structure (Aout; Bout = 0), it is possible to obtain an array of relative values of the amplitudes in each of the PC layers by numerical calculation.

Transmittance coefficient:

$$T = 1 - |\frac{B_0}{A_0}|^2 \quad (11)$$

These calculations also made it possible to calculate the density of photon states in the layered structure. The most complete review of the features and a description of the method for calculating such an instrument as the density of photon states is disclosed in [27]–[30], which is the main quantity that determines the dynamics of radiation in a structured dielectric medium.

Knowing the states of photons in a photonic crystal, one can describe the processes of interaction of bound and free electrons with their own radiation field. The point is that this plays an essential role in describing the emission spectra of atoms in photonic crystals. Such processes, which, in particular, lead to a Lamb shift of the spectral lines of atoms, should be very significant at the frequencies of virtual photons in the band gap due to the trapping of radiation of the corresponding frequency. There is a direct relationship between the density of photonic states and the probability of quantum processes, which is described by the "Fermi golden rule".

In [30], a formula was proposed for determining the density of photon states in periodic media:

$$\rho_\omega = \frac{\frac{1}{2L_\Sigma}\int_0^{L_\Sigma}[\epsilon(\omega)|E_\omega|^2 + \frac{c^2}{\omega^2}|\frac{\partial E_\omega}{\partial z}|^2]\partial z}{c|E_\omega^I|^2} \quad (12)$$

Where LΣ is the total thickness of the structure, EωI is the amplitude of the incident wave, Eω is the amplitude of the

electric component of the EM field, $\epsilon\omega(z)$ is the dielectric constant from the coordinate, c is the speed of light in vacuum. The energy of the luminous flux U_N for an isotropic layer can be determined as:

$$U_N = \int_0^{L_\Sigma} I_N(x)S\frac{n_N^*}{c}\partial x \quad (13)$$

Where S is the area; - the time the photon passes through the layer.

Having the values of both opposite amplitudes (A_N and B_N), the light intensity in the layer is calculated:

$$I_N(x) = \varepsilon_0 c n_N^*(|A_N|^2e^{-\alpha_Nx} + |B_N|^2e^{-\alpha_N(L_N-x)}) \quad (14)$$

From equations 13 and 14:

$$U_N = \varepsilon_0\frac{(n_N^*)^2}{2}S(|A_N|^2 + |B_N|^2)\frac{(1 - e^{-\alpha_NL_N})}{\alpha_N} \quad (15)$$

where α_N is the absorption coefficient in the layer.

Due to the peculiarity of the transfer matrix method, which implies a constant value equal to 1 for the amplitude of the outgoing radiation, a formula for the radiation flux incident on the first layer is obtained:

$$I_{in} = \frac{\varepsilon_0 c n_0}{2k_T} \quad (16)$$

In the case of an experiment, for a more comfortable comparison, its value is equated to one. Then the normalization takes place according to the basic parameters of the layers, which are the thickness and refractive index. As a result, we obtain the photon flux energy of the entire photonic crystal:

$$U_\Sigma = \frac{2k_T}{\epsilon_0 c n_0}\sum_N U_N =$$

$$= \frac{Sk_T}{\epsilon_0 c n_0}\sum_N[(|A_N|^2 + |B_N|^2)\frac{(1 - e^{-\alpha_NL_N})}{\alpha_N}(n_N^*)^2] \quad (17)$$

Average density by volume:

$$\rho_\Sigma = \frac{U_\Sigma}{V} = \frac{k_T}{c n_0 L_\Sigma}\sum_N[(|A_N|^2 + |B_N|^2)\frac{(1 - e^{-\alpha_NL_N})}{\alpha_N}(n_N^*)^2] \quad (18)$$

Energy density for the same volume in the absence of a photonic crystal from equation 4 with the condition of a single incident flow passing in one direction:

$$\rho_0 = \frac{n_0}{c} \quad (19)$$

Relative energy density:

$$\rho = \frac{\rho_\Sigma}{\rho_0} = \frac{k_T}{L_\Sigma n_0^2}\sum_N[(|A_N|^2 + |B_N|^2)\frac{(1 - e^{-\alpha_NL_N})}{\alpha_N}(n_N^*)^2] \quad (20)$$

Not taking into account the damping factor through to the expression $\lim_{\alpha_N \to 0} \frac{(1-e^{-\alpha_N L_N})}{\alpha_N} = L_N$. Then:

$$\rho \approx \frac{k_T}{L_\Sigma n_0^2} \sum_N (|A_N|^2 + |B_N|^2) L_N n_N^2, \qquad (11a)$$

Having values of amplitudes for any wavelength, in fact, the dependence of the amount of radiation energy in an object depends on frequency.

III. RESULTS

When examining the samples with an electron microscope, a sufficiently low accelerating voltage was used and a low beam current does not distort the real structure. Figure 1 shows the results obtained from the surface of leaves and needles. The revealed structure consists of nanotubes with characteristic dimensions: 150 nm in diameter and 3-5 μm in length.
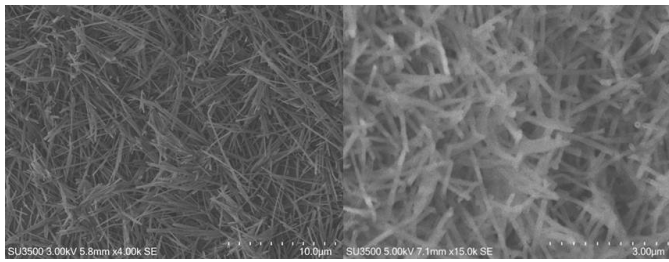

Fig. 1. SEM images of isolated wax layer samples. On the left is gray wheat. On the right is a blue spruce.

Blue spruce wax consists of nanotubes, while wheat wax consists of rods.

Polarization microscopy showed that most of the wax plates form large heterogeneous areas diffusing the light greatly. At the same time, domains from 1 to 4 microns in size are visible, located separately or in form of small conglomerates (Fig. 2). They have a blue (blue-green) colour (Fig. 2, a) in reflected light, and become pink in transmitted light (Fig. 2, b). In reflected light, the maximum brightness of the domain is observed in its center, which complies with the strongest colour of the domain in transmitted light. The observed irisation in reflected light indicates the presence of a PC structure.

Due to interesting scientific results in the field of studying PC with high dielectric contrast, the number of publications is growing rapidly every year. Structures with defects, which have found important practical applications in practice, including in nanophotonics and microelectronics [31] - [37], are of particular interest. A detailed classification of defects in such structures is considered in [31]. To interpret the experimental results, we considered two one-dimensional models consisting of tubes and rods. Tubes and rods in space are located parallel to each other and form a layered structure (Fig. 3, Left). When light is incident perpendicular to the plane in which the tubes are located, a periodic structure of two layers is obtained, where one layer is air with a refractive index of 1 and the second layer is wax with a refractive index of 1.46 (Fig. 3, Right).
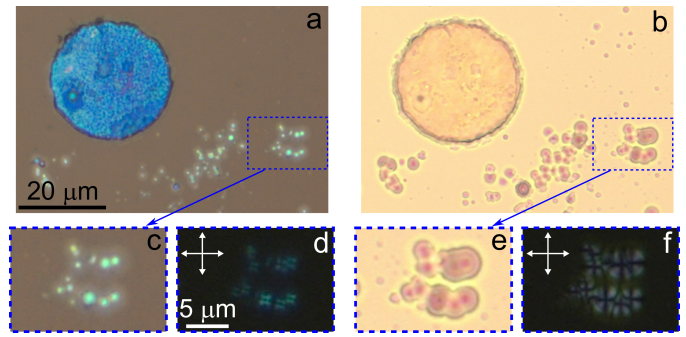

Fig. 2. Photographs of wax domains on a glass coverslip, taken in reflected (a,c,d), transmitted non-polarized light (b,e,f) and polarized light in the geometry of crossed polarizers (d and f). Enlarged area (upper row) of the photograph with domains and their conglomerates (lower row). The directions of the polarizers are indicated by double arrows.

In the tube model, one completely filled tube was used as a defect. The model with rods used a wax layer 2 times wider than all the others, which simulated 2 brazed rods.
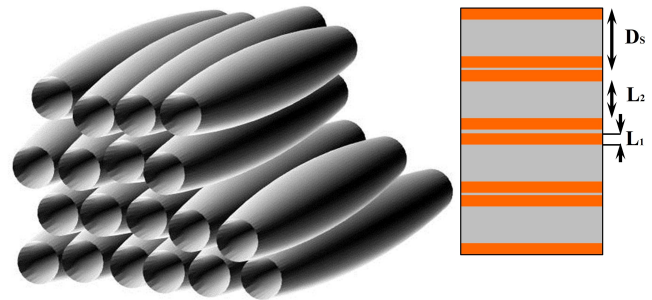

Fig. 3. On the left is a three-dimensional model of the arrangement of wax nanotubes. On the right is a one-dimensional periodic grating with the calculated parameters: Ds = 140 nm; L1 = 30 nm; L2 = 80 nm; N1 = 1.46; N2 = 1.

For the structures described above, the transmission spectra were calculated.

In addition, to consider a more natural model, the structure was calculated with random variations in nanotube diameters up to 15 per cent (Figure 4).

Figure 5 shows the spectrum of the density of photon states obtained from the main calculated characteristics of the transmission spectrum. In [38], a direct relationship was established between the density of photon states and fluorescence. The fluorescence spectrum obtained from the images of blue spruce is shown in Figure 6. Comparison of Figures 5 and 6 shows their coincidence. Good agreement between the results indicates that the calculations are correct.

The transmission spectrum allows obtaining the corresponding spectra of the density of photon states (Figure 5). According to [38], the density of photon states is directly proportional to the fluorescence spectra. In fig. 6 shows the fluorescence plots obtained from isolated layers of blue spruce and blue-gray wheat wax.

Figures 5 and 6 show that the graphs of the density of states of photons and the graph of fluorescence completely coincide,
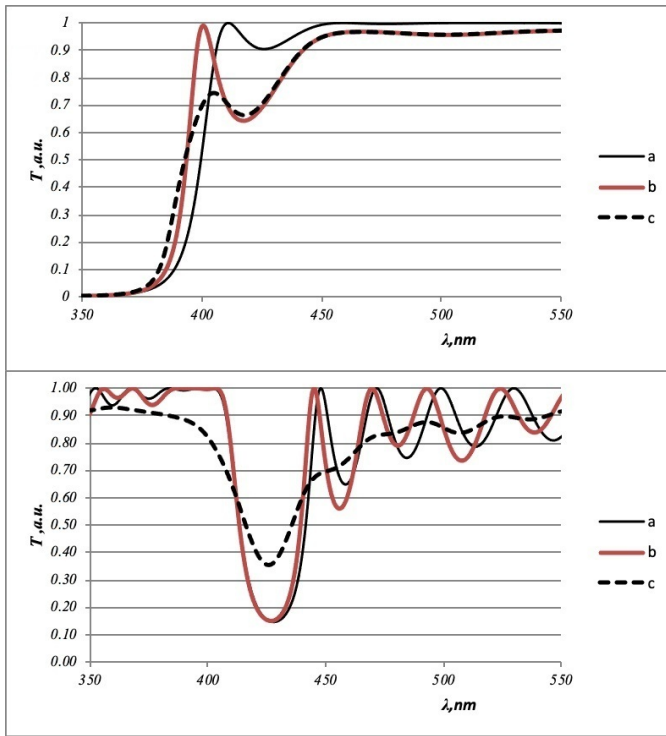
Fig. 4. Calculated transmission spectra. (Above) a periodic structure taking into account the hollow space of the tubes. (Bottom) A periodic structure consisting of rods. (a) a defect-free layered structure (b) a layered structure with a defect (c) a disordered layered structure with a defect.
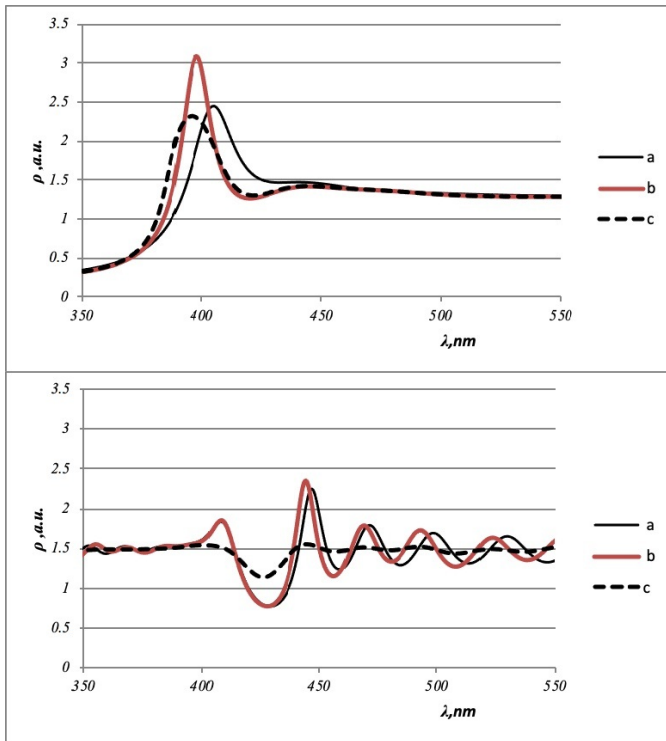

Fig. 5. Calculated spectra of the density of photon states. (Above) a periodic structure taking into account the hollow space of the tubes. (Bottom) A periodic structure consisting of rods. (a) a defect-free layered structure (b) a layered structure with a defect (c) a disordered layered structure with a defect.
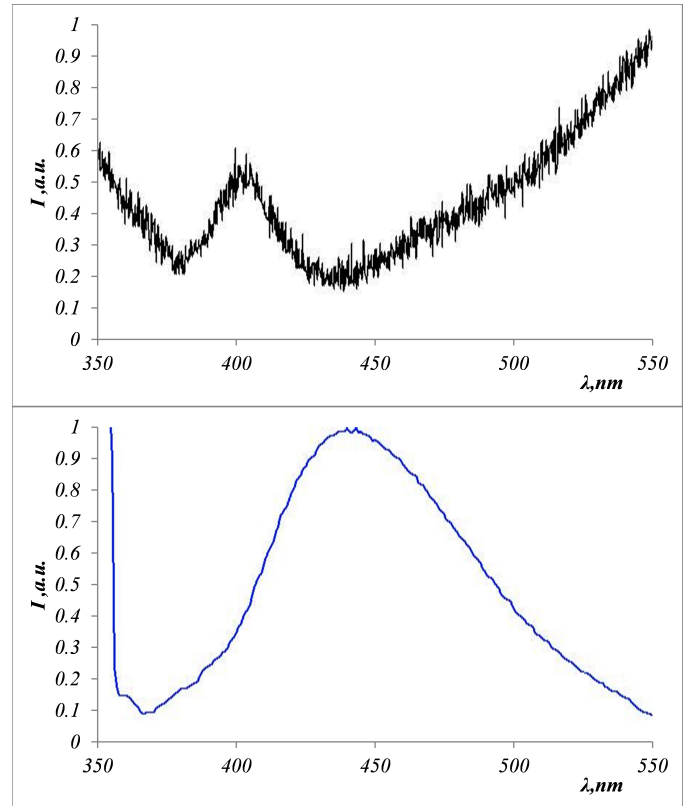

Fig. 6. Experimentally obtained fluorescence spectrum. (Top) Tubules. (Bottom) Rods.

which indicates the convergence of the calculation.

An important result was obtained in the study of the effect of defects on the density of photonic states. Figure 5 shows that a structure consisting of nanotubes, in which the rod was used as a defect, has a higher density of photon states at the defect than at the edges of the band-gap.

IV. DISCUSSION

Nearly every plant that exists in the world is covered with a specific layer of epicuticular wax. This wax, due to its optical characteristics, works as a barrier between the light and the plant. Our research aimed at studying these optical characteristics in order to understand which wavelengths can pass through it and which are absorbed and reflected. Structural characteristics of epicuticular wax were studied in a number of research articles [21], [22], [39]. The results of our study of morphological characteristics are in good agreement with the research findings mentioned in [21], [22], [39]. In particular, it was discovered that the structural units of wax are nanotubes and nanorods with an external diameter of 140–160 nm. A characteristic feature of the wax is that it consists of a complex mixture of long chain aliphatic compounds, which can be classified according to the type of functional groups, structure and distribution of homologs [4]. Moreover, cyclic compounds can be discovered in various amounts. As research [4] shows, wax units can also form anisotropic

crystals due to their ability to self-organize. A detailed study of the self-organization mechanisms of wax structural units was carried out in [13]. It suggested extracting the wax layer using chloroform and then precipitating it on various substrates to grow structural complexes. Wax structures were grown on silicon, graphite and paraffin. The experiments showed that the morphology of recrystallization on paraffin is similar to that on the surface of plants, although a significant difference regarding tubes orientation and their spatial distribution was observed on other substrates. Koch in [13] provides a detailed study of the wax tubes growth mechanism. Rods form ring structures. These circular structures formation was caused by simultaneous dissolution of one end of the rod, while the other end began to form a curved line. When this curved line closed in a circle, the waxes began to grow in height. Koch et al. [13] also demonstrated vertical orientation of the tubes on highly oriented pyrolytic graphite (HOPG). Using atomic force microscopy, they observed continuous tube growth after applying 10 mcl of a drop (conc. 1.5 mg /ml) to the surface of the HOPG. They also observed an increase in the contact angle from 88° to 129° after 14 days of wax recrystallization on HOPG. This means an increase in the hydrophobicity of wax structures. An interesting study on the effect that the concentration of a solution and its impurities has on the growth rate was presented in [14]. Time dependence of the wax tubes formation after recrystallization from various solutions based on chloroform on the HOPG surface at room temperature was studied using atomic force microscopy (magnetic alternating current mode). The formation process was observed using a series of successive images. The tubes that are oriented vertically grow following the rod > ring > tube scheme. Various factors, such as different concentrations of wax in chloroform, the presence of water or salts $[(NH_4)_2SO_4, NH_4NO_3]$ or a salt/water mixture in solution, that can influence the growth rate and orientation of the tubes, were also studied. It was discovered that difference in concentrations of wax do not have any effect on the growth rate or orientation of the tubes in any of the solutions. However, it was noted that water significantly increased tubes formation growth rate, while salt did not affect the growth rate or orientation of the tubes. We must add that photonic structures may have a certain effect on internal cells in a wax layer by creating initial resonance for a light wave that passes through a plant. The effective fluorescence discovered as part of the study can be well explained by the results of [38], in which the relationship between the fluorescence line and the density of photon states is described. Thus, talking about a tube, we may say that the internal distances between the walls of the tubes stay the same, showing equivalency to maintaining short-range order. At the same time, the distances between rods are disordered. That is why structures consisting of rods are more inclined to disorder, as Figures 4 and 5 show.

V. Conclusion

A study of the wax structures of blue spruce and gray wheat was carried out. It was found that they form crystalline long-period structures. When comparing the waxes of spruce and wheat, there is a clear difference, both in experimental and theoretical parameters. With different optical and morphological characteristics, they have the same most important characteristic feature. Under the influence of ultraviolet radiation in the visible region, intense fluorescence appears corresponding to the peaks of the density of photon states.

References

[1] J. M. Weaver, G. Lohrey, P. Tomasi, J. M. Dyer, M. A. Jenks and K. A. Feldmann, "Cuticular wax variants in a population of switchgrass (Panicum virgatum L.)," Industrial Crops and Products, vol. 117, pp. 310-316, 2018.

[2] D. A. Reicosky and J. M. Hanover, "Physiological Effects of Surface Waxes: I. Light Reflectance for Glaucous and Nonglacous Picea pungens," Plant Physiol, vol. 62, pp. 101-104, 1978.

[3] C. A. Harrington and W. C. Carlson, "Morphology and accumulation of epicuticular wax on needles of Douglas-fir (Pseudotsuga menziesii var. menziesii)," Northwest Science, vol. 89, no. 4, pp. 401-408, 2016.

[4] S. Dragota and M. Riederer, "Comparative study on epicuticular leaf waxes of Araucaria araucana, Agathis robusta and Wollemia nobilis (Araucariaceae)," Australian Journal of Botany, vol. 56, no. 8, pp. 644-650, 2008.

[5] J. Guo, W. Xu, X. Yu, H. Shen, H. Li, D. Cheng, A. Liu, J. Liu, C. Liu, S. Zhao and J. Song, "Cuticular Wax Accumulation Is Associated with Drought Tolerance in Wheat Near-Isogenic Lines," Front. Plant Sci, vol. 7, no. 1809, 10, 2016.

[6] H. Bi, N. Kovalchuk, P. Langridge, P. J. Tricker, S. Lopato and N. Borisjuk, "The impact of drought on wheat leaf cuticle properties," BMC Plant Biology, vol. 17, no. 85, pp. 1-13, 2017.

[7] K. Koch, W. Barthlott, S. Koch, A. Hommes, K. Wandelt, W. Mamdouh, S. De-Feyter and P. Broekmann, "Structural analysis of wheat wax (Triticum aestivum, c.v. 'Naturastar' L.): from the molecular level to three dimensional crystals," Planta, vol. 223, pp. 258-270, 2005.

[8] G. Bianchi, "Plant waxes. In Waxes: Chemistry, molecular biology and functions," The Oily Press, pp. 175-222, 1995.

[9] W. Barthlott, C. Neinhuis, D. Cutler, F. Ditsch, I. Meusel, I. Theisen and H. Wilhelmi, "Classification and terminology of plant epicuticular waxes," J. Bot. Linnean Soc., vol. 126, pp. 237-260, 1998.

[10] W. Barthlott, "Scanning electron microscopy of the epidermal surface in plants. Scanning electron microscopy in taxonomy and functional morphology," Syst.Assoc. Spec., vol. 41, pp. 69-94, 1990.

[11] T. J. Walton, "Waxes, cutin and suberin," London: Academic, pp. 105-158, 1990.

[12] L. Kunst and A.S. Samuels, "Biosynthesis and secretion of plant cuticular wax," Prog. in Lipid Res., vol. 42, pp. 51-80, 2003.

[13] K. A. Koch, A. Dommisse and W. Barthlott, "Chemistry and Crystal Growth of Plant Wax Tubules of Lotus (Nelumbo nucifera) and Nasturtium (Tropaeolum majus) Leaves on Technical Substrates," Crystal growth and design, vol. 6, no. 11, pp. 2571-2578, 2006.

[14] S. K. Dora, K. Koch, W. Barthlott and K. Wandelt, "Kinetics of solvent supported tubule formation of Lotus (Nelumbo nucifera) wax on highly oriented pyrolytic graphite (HOPG) investigated by atomic force microscopy," Beilstein J. Nanotechnol., vol. 9, pp. 468-481, 2018.

[15] S. K. Dora, "Real Time Recrystallization Study of 1, 2 Dodecanediol on Highly Oriented Pyrolytic Graphite (HOPG) by Tapping Mode Atomic Force Microscopy," World Journal of Nano Science and Engineering, vol. 7, pp. 1-15, 2007.

[16] S. K. Dora and K. Wandelt, "Recrystallization of tubules from natural lotus (Nelumbo nucifera) wax on a Au(111) surface," Beilstein J. Nanotechnol., vol. 2, pp. 261-267, 2011.

[17] E. Poinern, X.T. Le and D. Fawcett, "Superhydrophobic nature of nanostructures on an indigenous Australian eucalyptus plant and its potential application, Nanotechnology, Sci. and App., vol. 4, pp. 113-121, 2011.

[18] D. Lee, "Nature's Palette: The Science of Plant Color," Chicago: Univer-sity of Chicago Press, 2010.

[19] S. Vignolini, E. Moyroud, B. J. Glover and U. Steiner, "Analysing photonic structures in plants," Journal R. Soc. interface., vol. 10, no. 87, pp. 1-9, 2013.

[20] K. R. Thomas, M. Kolle, H. M. Whitney, B. J. Glover and U. Steiner, "Function of blue iridescence in tropical understorey plants," J. R. Soc. Interface, vol. 7, no. 53, pp. 1699-1707, 2010.

[21] H. J. Ensikat, C. Neinhuis and W. Barthlott, "Direct access to plant epicuticular wax crystals by a new mechanical isolation method," Int. J. Plant Sci., vol. 161, no. 1, pp. 143-148, 2000.

[22] H. J. Ensikat, M. Boese, W. Mader, W. Barthlott and K. Koch, "Crystallinity of plant epicuticular waxes: electron and X-ray diffraction studies," Chem. and Phys. of Lipids, vol. 144, pp. 45-59, 2006.

[23] E. R. Bukhanov, A. V. Shabanov, M. N. Krakhalev, M. N. Volochaev and Yu. L. Gurevich, "The effect of the structure on the optical properties of epicular blue spruce wax (Picea pungens)," Memoirs of the Faculty of Physics, vol. 5, 1950502-1, 2019.

[24] V. F. Shabanov, S. Ya. Vetrov and A. V. Shabanov, "Optics of real photonic crystals," Novosibirsk: SB RAS Publisher, 2005.

[25] A. V. Shabanov, M. A. Korshunov and E. R. Bukhanov, "Investigation of the electromagnetic field in one-dimensional photonic crystals with defects," Computer Optics, vol. 41, no. 5, pp. 680-686, 2017. DOI: 10.18287/2412-6179-2017-41-5-680-686.

[26] A. V. Shabanov, M. A. Korshunov and E. R. Bukhanov, "Features of the amplification of the electromagnetic field and the density of states of photonic crystal structures in plants," Computer Optics, vol. 43, no. 2, pp. 231-237, 2019. DOI: 10.18287/2412-6179-2019-43-2-231-237.

[27] N. Vats, S. John and K. Busch, "Theory of fluorescence in photonic crystals," Physical Review A., vol. 65, 43808, 2002.

[28] J. Schmidtkea and W. Stille, "Fluorescence of a dye-doped cholesteric liquid crystal film in the region of the stop band: theory and experiment," The European Physical Journal B., vol. 31, pp. 179-194, 2003.

[29] G. D'Aguanno, N. Mattiucci, M. Scalora, M. J. Bloemer and A. M. Zheltikov, "Density of modes and tunneling times in finite one-dimensional photonic crystals: A comprehensive analysis," Physical Review E., vol. 70, 16612, 2004.

[30] G. D'Aguanno, M. Centini, M. Scalora, C. Sibilia, Y. Dumeige, P. Vidakovic, J. A. Levenson, M. J. Bloemer, C. M. Bowden, J. W. Haus and M. Bertolotti, "Photonic band edge effects in finite structures and applications to x2 interactions," Physical Review E., vol. 64, 16609, 2001.

[31] S. V. Eliseeva, V. A. Ostatochnicov and D.I. Sementsov "Field and spectra of one-dimensional photonic crystal with inversion type defect," Computer Optics, vol. 36, no. 1, pp. 14-20, 2012.

[32] L. L. Doskolovich, D. A. Bykov, E. A. Bezus and V. A. Soifer, "Spatial differentiation of optical beams using phase-shifted Bragg grating," Opt. Lett., vol. 39, no. 5, pp. 1278-1281, 2014.

[33] D. A. Bykov, L. L. Doskolovich, E. A. Bezus and V. A. Soifer, "Optical computation of the Laplace operator using phase-shifted Bragg grating," Optics Express, vol. 22, no. 21, pp. 25084-25092, 2014.

[34] N. V. Golovastikov, D. A. Bykov, L. L. Doskolovich and E. A. Bezus, "Spatial optical integrator based on phase-shifted Bragg gratings," Optics Communications, vol. 338, pp. 457-460, 2015.

[35] Y. F. Nasedkina, S. V. Eliseeva and D. I. Sementsov, "Transformation of a Gaussian pulse when interacting with a one-dimensional photonic crystal with an inversion defect," Photonics and Nanostructures – Fundamentals and Applications, vol. 19, pp. 31-38, 2016.

[36] Yu. S. Dadoenkova, N. N. Dadoenkova, I. L. Lyubchanskii and D. I. Sementsov, "Reshaping of Gaussian light pulses transmitted through one-dimensional photonic crystals with two defect layers," Applied Optics, vol. 55, pp. 3764-3770, 2016.

[37] R. A. Abram, A. A. Greshnov, S. Brand and M. A. Kaliteevski, "A study of a phase formalism for calculating the cumulative density of states of one-dimensional photonic crystals," Journal of Modern Optics, vol. 64, no. 15, pp. 1501-1509, 2017.

[38] P. V. Dolganov, "Spectral features of cholesteric luminescence photonic crystal," JETP Letters, vol. 105, no. 10, pp. 616-620, 2017.

[39] K. Koch, W. Barthlott, S. Koch, A. Hommes, K. Wandelt, W. Mamdouh, S. De-Feyter and P. Broekman, "Structural analysis of wheat wax (Triticum aestivum, c.v. 'Naturastar' L.): from the molecular level to three dimensional crystals," Planta, vol. 223, pp. 258-270, 2006.